

High-temperature deformation behaviour of $\text{YBa}_2\text{Cu}_3\text{O}_{7-x}$

W.-J. KANG

Department of Materials Processing, Tohoku University, Sendai 980, Japan

S. HANADA

Institute for Materials Research, Tohoku University, Sendai 980, Japan

Y. WADAYAMA

Hitachi Research Laboratory, Hitachi, Ltd, Hitachi-shi, Ibarakiken, Japan

A. NAGATA

Department of Metallic Materials for Engineering, Mining College, Akita University, Akita 010, Japan

High-temperature compression tests were performed in air for $\text{YBa}_2\text{Cu}_3\text{O}_{7-x}$ polycrystals with grain sizes of 3 and 7 μm at various strain rates between 1.3×10^{-5} and $4 \times 10^{-4} \text{ s}^{-1}$ and at temperatures between 1136 and 1253 K. Steady state deformation appeared above 1203 K for both samples. A stress exponent of 1.3 and an activation energy of 150 kJ mol^{-1} were evaluated. The compression tests and microstructural observations revealed that there was a difference in deformation mechanism above and below 1203 K. The dominant mechanism was diffusional creep associated with grain-boundary sliding above 1203 K, and dislocation glide accompanied with grain-boundary sliding below 1203 K. The growth of anisotropic grains and their preferred arrangement were enhanced by deformation.

1. Introduction

Recently, it has been found that the development of strong texture in a $\text{YBa}_2\text{Cu}_3\text{O}_{7-x}$ polycrystal can be achieved by plastic deformation at high temperature [1]. The strongly textured polycrystal is expected to reduce the weak-link problem in grain boundaries and to improve the transport critical current density, J_c . Few data have been reported on the development of texture by plastic deformation of $\text{YBa}_2\text{Cu}_3\text{O}_{7-x}$ polycrystals, although plastic deformation behaviour has been investigated by several authors. Rabier and Denant [2, 3] have studied dislocations introduced by compression at room temperature and confirmed a glide system $[010] (001)$. Hatanaka and Sawada [4, 5] have found ferroelastic behaviour at about 473–623 K using a $\text{YBa}_2\text{Cu}_3\text{O}_{7-x}$ single crystal heated in a mechanically clamped state. Narita *et al.* [6] reported that the deformation twinning is induced in $\text{YBa}_2\text{Cu}_3\text{O}_{7-x}$ through reorientation of oxygen vacancy arrays at 533 K. They observed the change in intensity ratio of the $(200) + (006)$ to the (020) peak, I_a/I_b , by loading up to 300 MPa.

Suzuki and Takeuchi [7, 8] theoretically analysed the plasticity and deformability of superconducting ceramics based on Peierls stress and the number of operative slip systems, and predicted that the critical temperature for deformation is above 1090 K. Saka and co-workers [9, 10] observed the microstructure of samples deformed by micro-indentation at 923–1123 K. Some $\langle 100 \rangle$ dislocations were found

to dissociate into dislocations $1/2\langle 100 \rangle + 1/2\langle 100 \rangle$ at 923 K, whereas they did not dissociate at 1123 K.

Reyes-Morel *et al.* [11] have recently measured the flow stress in air at strain rates of 1×10^{-4} – $1 \times 10^{-6} \text{ s}^{-1}$ by compressive deformation at temperatures between 1073 and 1163 K. They found a stress exponent of 1.25 and activation energies of 1218 kJ mol^{-1} for higher temperatures, and 565 kJ mol^{-1} for lower temperatures with the transition at 1143 K. They suggested that the deformation is controlled by barium diffusion and speculated that the occurrence of two apparent activation energies is attributable to two different diffusion paths of the cations. Bussod *et al.* [12] reported results on the effects of temperature and strain rate on the plastic deformation of fully dense $\text{YBa}_2\text{Cu}_3\text{O}_{7-x}$ polycrystals. They found a stress exponent of 2.5 and an activation energy of 201 kJ mol^{-1} in air between 1023 and 1223 K at strain rates between 1×10^{-4} and $1 \times 10^{-6} \text{ s}^{-1}$. Stumberg *et al.* [13] measured the plastic deformation of 99% dense polycrystals under various oxygen partial pressures, $P(\text{O}_2)$, at temperatures between 1143 and 1253 K and strain rates between 5×10^{-6} and $4 \times 10^{-5} \text{ s}^{-1}$. They found a stress exponent of nearly one and an activation energy of 600 – 800 kJ mol^{-1} , dependent on oxygen partial pressure. Moreover, it has been shown [14] that steady-state creep rate can be expressed as a function of flow stress, grain size and temperature. These recent results

on high-temperature deformation behaviour remain conflicting. In order to control the textures of $\text{YBa}_2\text{Cu}_3\text{O}_{7-x}$ by plastic deformation, a further study is required for high-temperature deformation.

In this investigation, stress-strain curves are presented for both 3 and 7 μm grain-size specimens compressed at a constant crosshead speed at temperatures from 1136–1253 K. The stress exponent and activation energy were also investigated. Both the compression tests and microstructural observations revealed that there is a difference in deformation mechanism above and below 1203 K.

2. Experimental procedure

Ceramic samples of $\text{YBa}_2\text{Cu}_3\text{O}_{7-x}$ were prepared by the solid-state reaction method as described previously [15]. After pelletizing at 100 MPa, the pellet was sintered for 10–50 h at 1203 K in flowing oxygen and slowly cooled at 1 K min^{-1} to room temperature.

Samples with different grain sizes of 3 and 7 μm were used in this study. The samples had about 88 % theoretical density and a critical temperature (T_c) of about 90 K. X-ray diffraction revealed that the samples consisted of a single $\text{YBa}_2\text{Cu}_3\text{O}_{7-x}$ phase.

The compression samples of dimensions $3.2 \times 3.2 \times 6.4 \text{ mm}^3$, were cut from the sintered pellets using a diamond saw without water and were polished with lapping tape no. 6000 (Fuji Film LT-C6000). The compression tests were performed in air at a constant crosshead speed using an Instron-type testing machine equipped with a high-temperature furnace at 1136–1253 K. The stress was transmitted to the

sample by two SiC rods. A ceramic chip made of $\text{Al}_2\text{O}_3 + \text{ZrO}_2$ was set between a sample and the SiC rods and a thin gold foil (10 μm thick) was inserted between the sample and ceramic chips to prevent chemical reactions. The samples were heated in air at a rate of 4.5 K min^{-1} from room temperature to the test temperature. After testing, the samples were slowly cooled at a rate of 2 K min^{-1} to room temperature, because rapid cooling produces cracking owing to stress caused by anisotropic contraction [16, 17].

Both dynamic and static grain growth on deformation were examined with two kinds of samples; one was a compressed sample for dynamic grain growth and the other was an annealed sample, which was placed beside a compressed sample during compression testing, for static grain growth. The deformed samples were cut parallel and perpendicular to the compression axis for optical microscopy. Thin foils for transmission electron microscopy (TEM) were prepared by cutting a compressed sample perpendicular to the compression axis, mechanical polishing to 50–80 μm and then ion thinning. The foils were observed in a Jeol JEM-2000 EX electron microscope equipped with a goniometer stage allowing $\pm 45^\circ$ tilt in two orthogonal directions. The grain size was measured as accurately as possible by the conventional mean linear intercept method [18], counting at least 200 grains in each case. This material has very anisotropic grains with large aspect ratio. Therefore, the linear intercept was measured in two orthogonal directions on each plane, one parallel plane and the other perpendicular plane to the loading axis. The geometrical mean of these values was used to calculate the grain size.

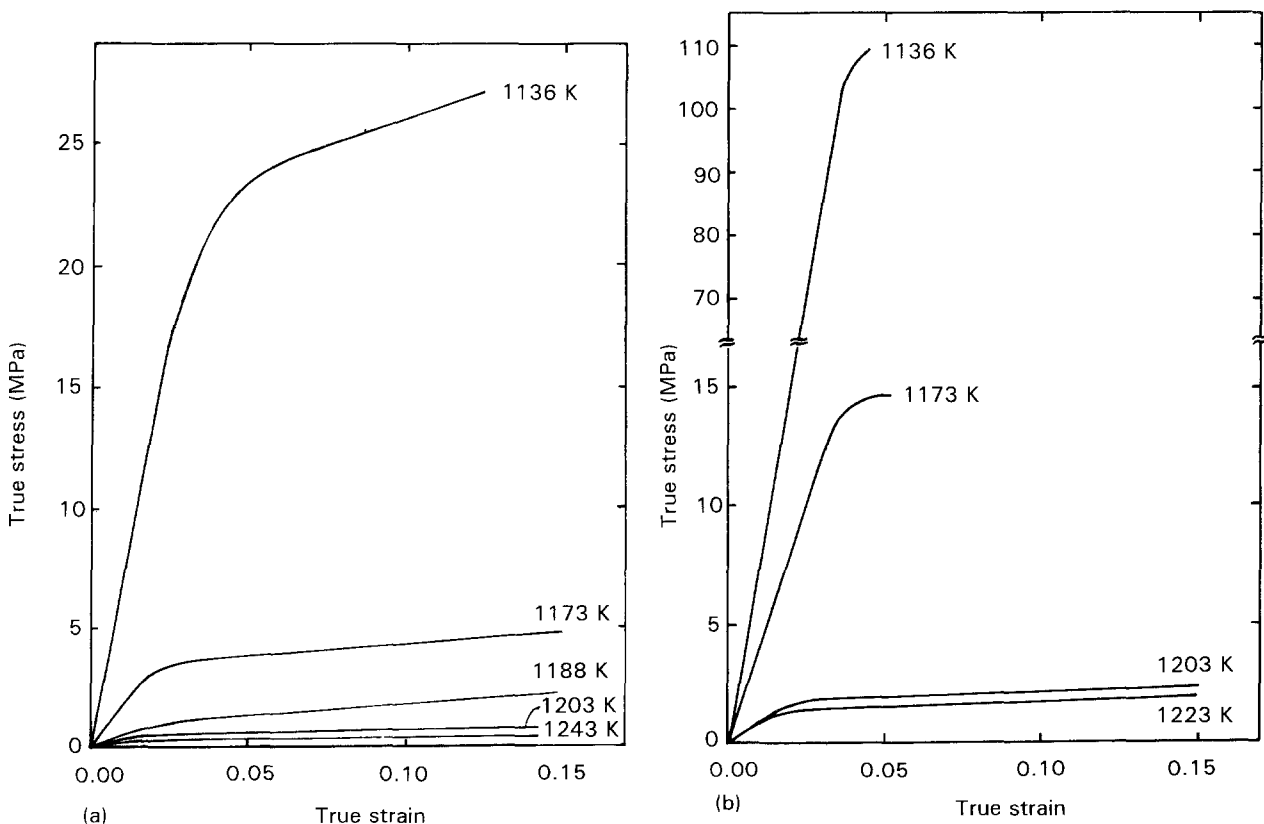


Figure 1 Stress-strain curves at 1136–1243 K for samples with grain sizes of (a) 3 μm , (b) 7 μm . $\dot{\epsilon} = 1.3 \times 10^{-5} \text{ s}^{-1}$.

Density was determined by Archimedes' method after coating the sample with viscous wax.

3. Results

Fig. 1a and b shows the stress-strain curves at 1136–1243 K for the samples with grain sizes of 3 and 7 μm , respectively. Steady-state deformation appeared above 1203 K for both samples. Steady-state stress is defined by a zero work-hardening rate [19] and is used as all terms of stress in this paper. An increase in density from 88 % to 95 % theoretical value was observed after plastic deformation to 40 % strain. Such a phenomenon has also been reported in previous works [8, 9]. Because macrocracking occurred in the samples with high flow stress, compression tests were interrupted at small strains. Fig. 2 shows plots of the logarithm of steady-state stress as a function of T^{-1} for a constant strain rate of $1.3 \times 10^{-5} \text{ s}^{-1}$. From the slope of the straight lines, activation energies are determined to be approximately 150 kJ mol^{-1} , independent of grain size. These results are not in accordance with those of previous workers [11–14].

The strain-rate sensitivity of steady-state stress at constant temperatures 1203, 1223 and 1243 K is shown in Fig. 3. The results at temperatures from 1203–1243 K give a stress exponent with a magnitude of 1.3 ± 0.1 . This agrees with that reported earlier [11–14], in which diffusional creep was suggested to be the dominant deformation mechanism in $\text{YBa}_2\text{Cu}_3\text{O}_{7-x}$ polycrystals.

TEM observations were performed with the compressed samples to investigate the microstructural

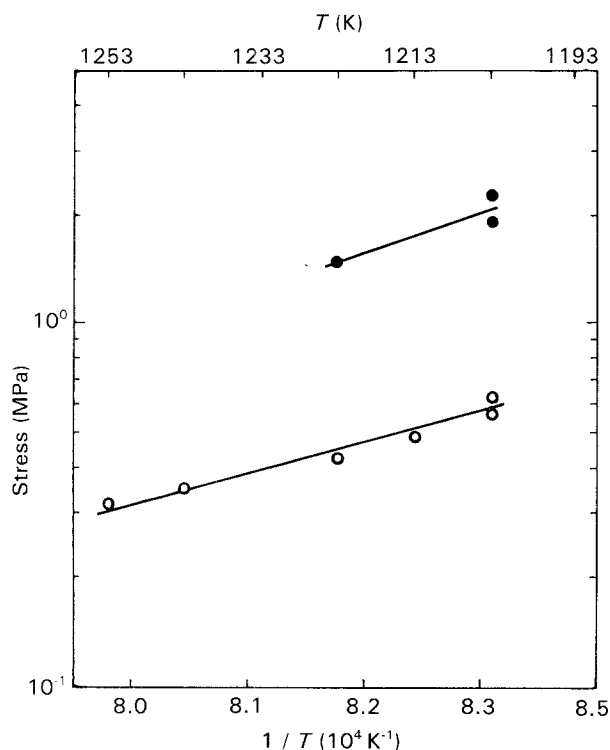


Figure 2 Plots of the logarithm of steady-state stress as a function of T^{-1} for an initial strain rate of $1.3 \times 10^{-5} \text{ s}^{-1}$ and grain sizes of (○) 3 μm and (●) 7 μm .

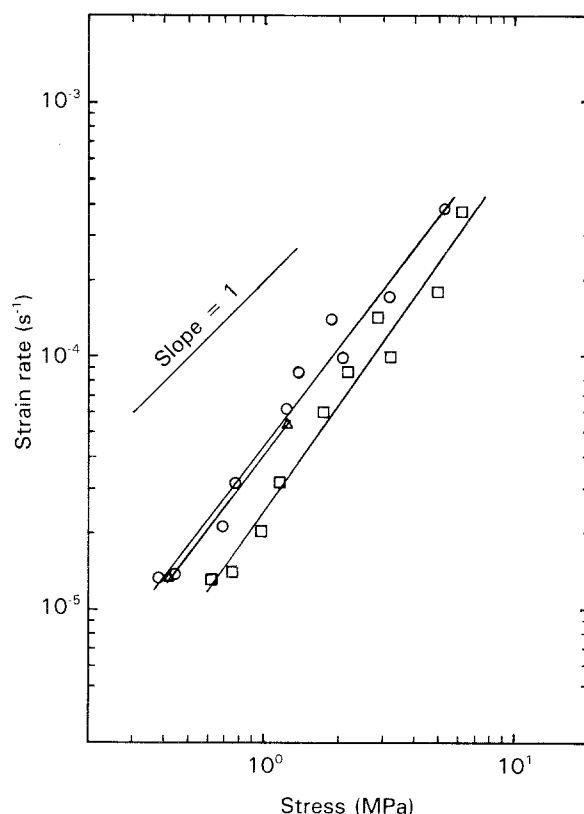


Figure 3 Strain-rate sensitivity of steady-state stress at (□) 1203, (△) 1223 and (○) 1243 K, for a grain size of 3 μm .

characteristics of the deformation. Typical microstructures of 15 % strained samples at 1136, 1173 and 1243 K are shown in Fig. 4a–c, respectively. The main feature of Fig. 4a and b is the presence of a high density of dislocations within the grains. The density of dislocations at 1136 K was higher than that at 1173 K. A similar dislocation structure was reported earlier [20] in the sample deformed by the indentation experiment at 1123 K. On the contrary, the lack of dislocations within most grains was evidently confirmed in the samples compressed at high temperatures such as 1203 and 1243 K. A typical example is shown in Fig. 4c. Only a few isolated dislocations were detected by repeated tilting experiments under various diffraction conditions. By using the $g \cdot b = 0$ criterion for invisibility, the Burgers vector of dislocations in samples deformed at 1136 K was determined. As shown in Fig. 5, the configuration of the dislocation in the sample deformed at 1136 K is found to be out of contrast only for $g = 200$ and this result is consistent with a $[010]$ Burgers vector. The $[010](001)$ glide system is considered to be operative.

Figs 6 and 7 show optical micrographs of statically annealed samples and deformed samples, respectively. The grain size increases with annealing time. Furthermore, it is evident that grain growth is enhanced by deformation and is accompanied by development of strong anisotropy in grain shape and preferred arrangement. Fig. 8 shows the static and dynamic grain growth with annealing time, indicating that dynamic grain growth occurs more rapidly than does static grain growth.

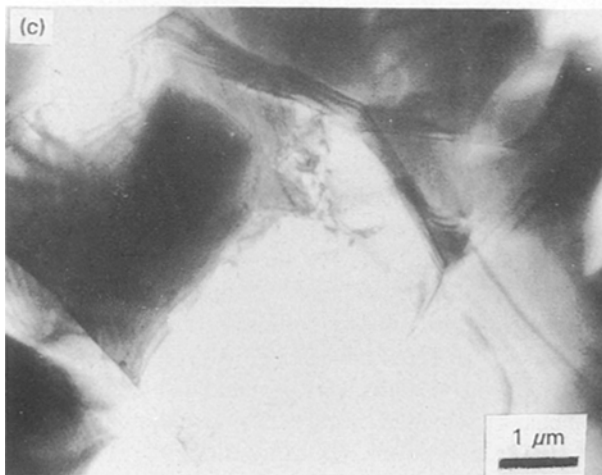
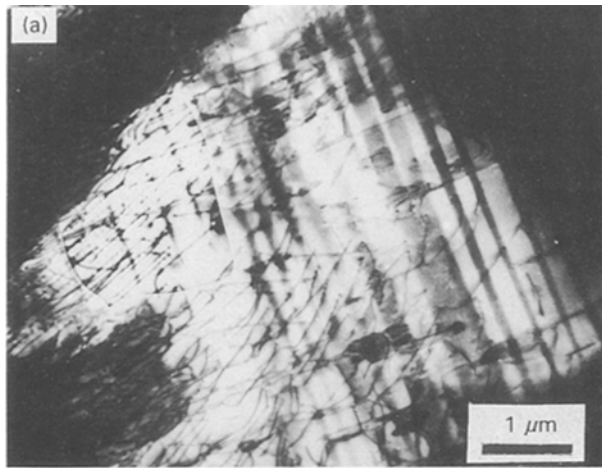


Figure 4 Typical TEM microstructures of 15% strained samples at (a) 1136 K, (b) 1173 K, and (c) 1243 K.

4. Discussion

The present TEM observations have revealed that there exist no discernible dislocations in the deformation microstructure above 1203 K, see Fig. 4c. In addition, the stress exponent of $n = 1.3 \pm 0.1$ is obtained above 1203 K. These results suggest that the high-temperature deformation is mainly controlled by diffusional creep. However, it is not clear whether or not the low activation energy, 150 kJ mol^{-1} , is reasonable for the diffusional creep, because no data on cation self-diffusion in $\text{YBa}_2\text{Cu}_3\text{O}_{7-x}$ are available.

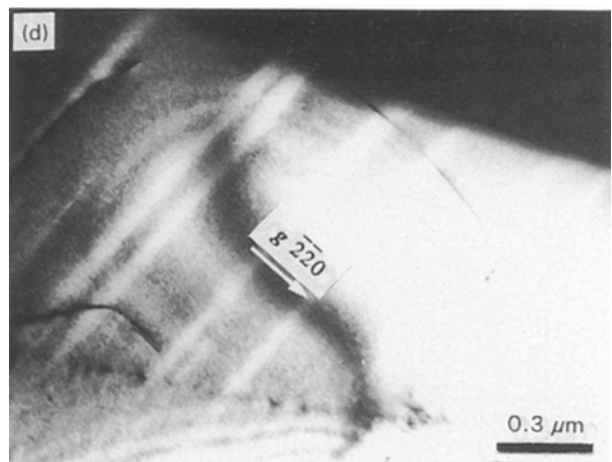
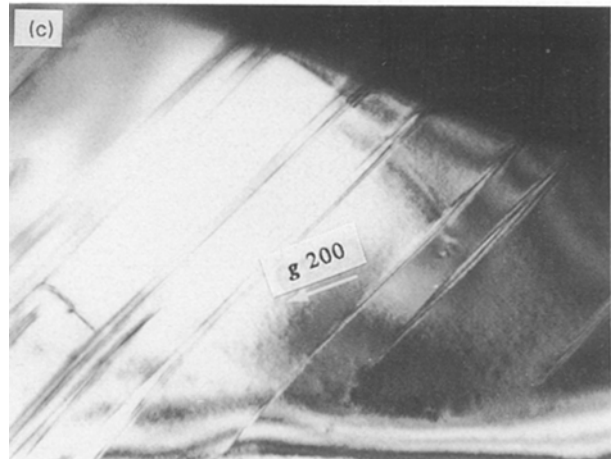
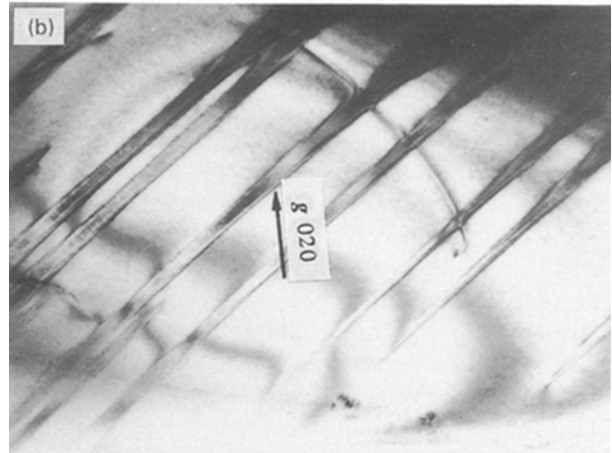
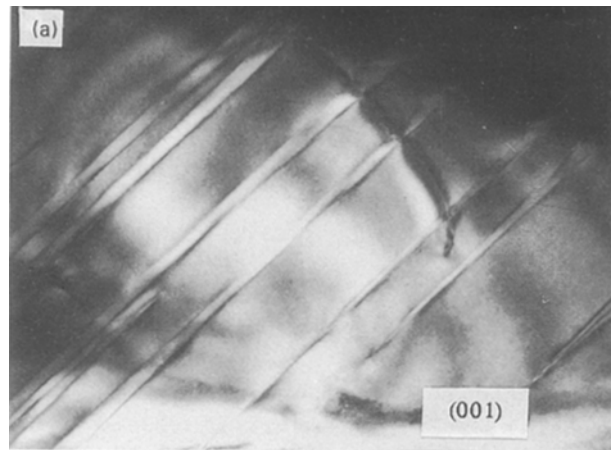


Figure 5 Dislocation contrast in the sample deformed at 1136 K: (a) $g = 001$, (b) $g = 020$, (c) $g = 200$, and (d) $g = 220$.

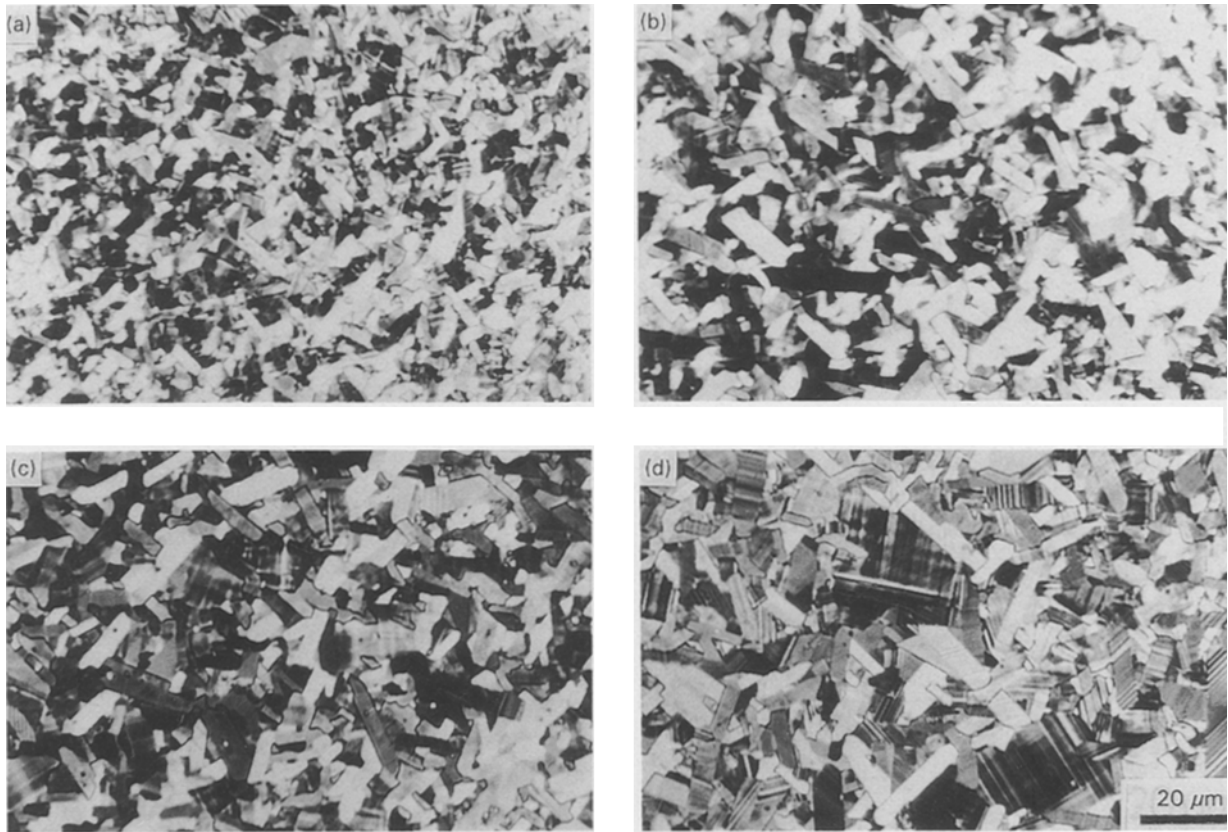


Figure 6 Optical micrographs of statically annealed samples for (a) 8.65 ks, (b) 15.3 ks (c) 29.8 ks and (d) 44.6 ks.

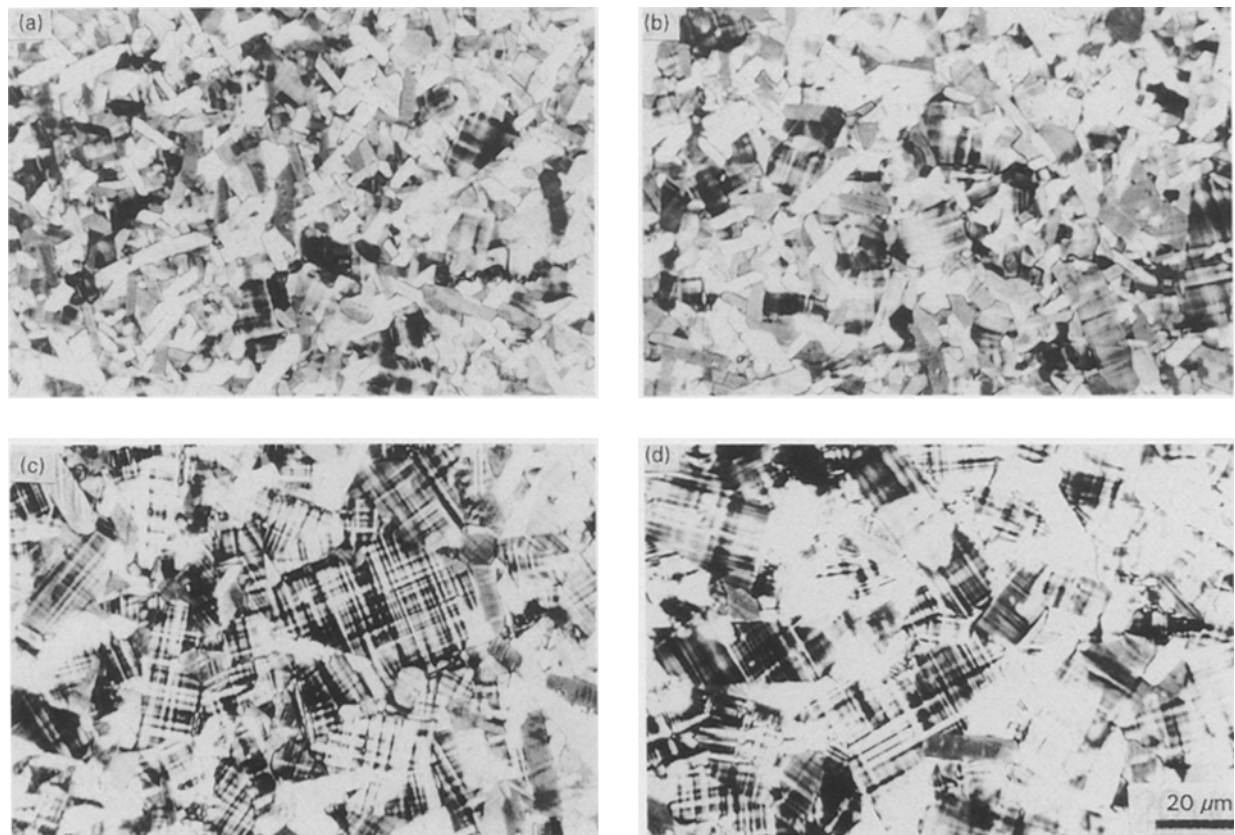


Figure 7 Optical micrographs of deformed samples: (a–d) micrographs of the planes perpendicular to the compressed axis; (e–h) micrographs of the planes parallel to the compressed axis. The time required to attain (a, e) 10 %, (b, f) 20 %, (c, g) 40 % and (d, h) 55 % strain was 8.65, 15.3, 29.8 and 44.6 ks, respectively. The annealing time in Fig. 6 is determined from this result.

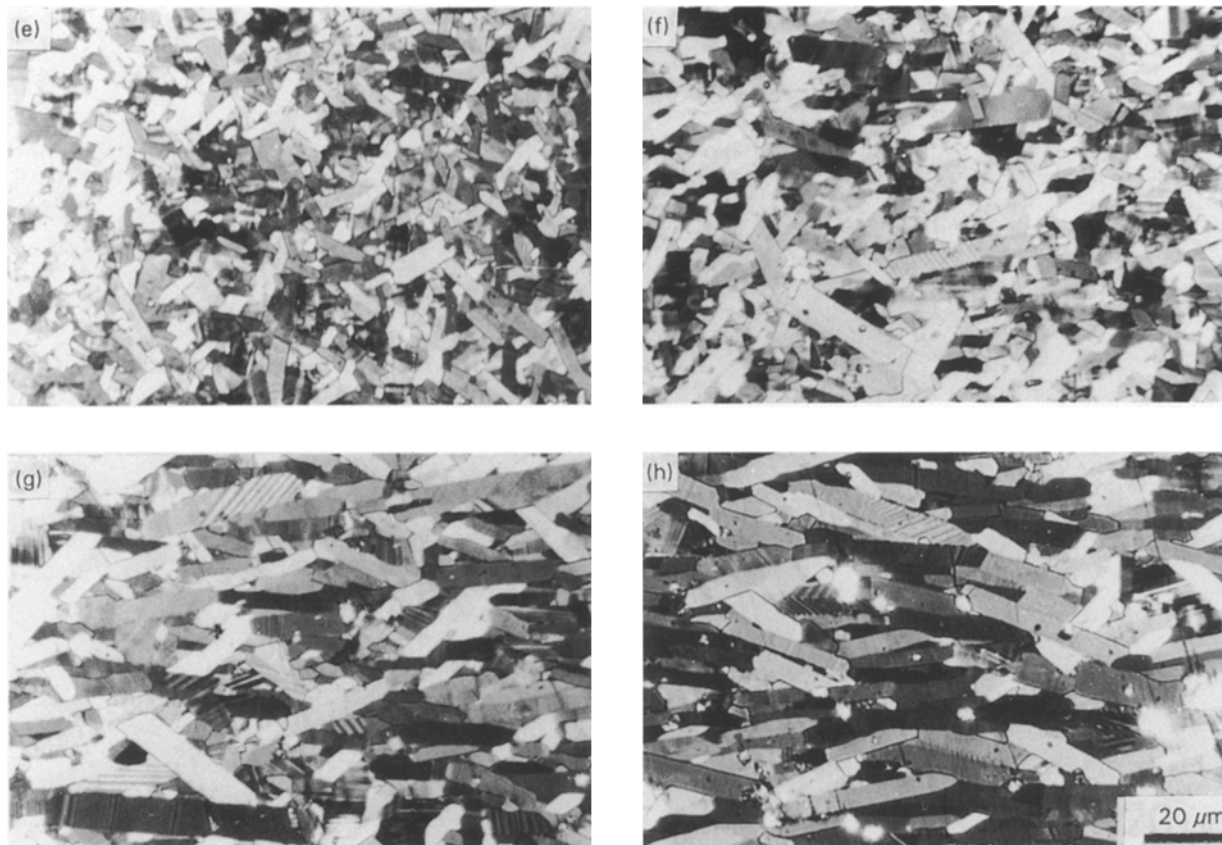


Fig. 7 continued

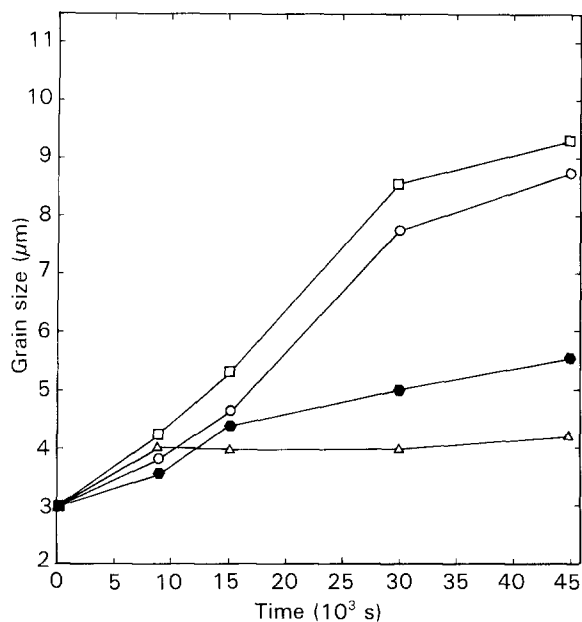


Figure 8 (○) Static and (○ □ △) dynamic grain growth with annealing time at 1203 K. Compression axis: (○) perpendicular; (□) parallel, length direction; (△) parallel, width direction.

It has been reported that the activation energy for high-temperature deformation of polycrystalline $\text{YBa}_2\text{Cu}_3\text{O}_{7-x}$ depends on oxygen partial pressure, $P(\text{O}_2)$ [13, 14]. However, even if this is taken into consideration, there is a large difference in activation energy between this study and the previous studies by von Stumberg *et al.* [13] and Goretta *et al.* [14].

We observed steady-state deformation to over 40 % strain above 1203 K and the development of strong anisotropy in grain shape, while they observed steady-state deformation to over 10 % strain at low temperatures below 1203 K and no change in distribution and texture of anisotropic grains in spite of considerable increase in grain size.

In general, steady-state deformation has been found under such conditions that high-temperature deformation is controlled by dislocation creep, diffusional creep, grain-boundary sliding or dynamic recrystallization. Grains in a sample deformed by dislocation creep and diffusional creep are elongated, depending on stressed direction. The size and shape of grains are unchanged in a sample deformed by grain-boundary sliding, such as a superplastically deformed, fine-grained sample. Grain refinement usually occurs in a sample deformed by dynamic recrystallization. Therefore, it seems to be difficult to explain the mechanism of the steady-state deformation observed by von Stumberg and colleagues [13, 14] in relation to microstructural changes. On the other hand, Kaibyshev *et al.* [21] have recently reported that $\text{YBa}_2\text{Cu}_3\text{O}_{7-x}$ exhibited superplasticity-like deformation behaviour in compression tests at 1173 and 1203 K. They showed stress-strain curves with a peak stress followed by steady-state deformation and observed many pores and cracks after deformation. They considered that these cavities were formed to accommodate intense grain-boundary slipping. We also observed that cracks were introduced in a sample deformed at temperatures below 1203 K to over a

strain at a peak stress and macroscopic cracking was caused by these cracks on further straining. Therefore, it is not believed that these cracks are introduced as an accommodation process of superplastic deformation based on grain-boundary sliding.

The present TEM observations indicating the existence of a high density of dislocations (Fig. 4a, b) and the increment of work-hardening rate suggest that the deformation below 1203 K (Fig. 1) is controlled by dislocation slip. The determined Burgers vector [010] does not satisfy the von Mises criterion [22], indicating that a polycrystal to undergo a general change of shape by slip requires the operation of five independent slip systems. Considerable plastic flow was, however, observed below 1203 K without macrocracking, indicating that a plastic deformation mode other than dislocation slip, e.g. deformation twinning, grain-boundary sliding or grain-boundary migration, is operative. Deformation twinning has been reported in the temperature range 473–623 K [4–6], but not in the high-temperature range where the oxide has tetragonal structure. In fact, we did not observe any deformation twins in this study. Grain-boundary sliding or grain-boundary migration, as well as dislocation slip, is likely to occur, because significant changes in optical microstructure are observed after deformation. Furthermore, the observed plastic flow may be partly due to microcracking at grain boundaries, because macrocracking appeared at smaller strain in the sample compressed below 1203 K.

Thus, activation energy should be measured by using samples indicating steady-state deformation to over 40% strain without a peak stress. This experimental condition can be achieved above 1203 K at 1.3×10^{-5} . The low activation energy may be expected from the experimental observations that oxygen vacancies [23–25] and lattice parameter c [26–29] increase rapidly with increasing temperature. The anomalous increase in lattice parameter c has been explained in terms of the creation of vacancies in the O(4) sites that separate the copper and oxygen planes and chains. That is, the creation of the O(4) vacancies in the 0, 0, z positions leads to a decrease in the net electrostatic attractive force in the z direction. If this is the case, cation diffusion along the c plane may become easy and, as a result, the activation energy may be lowered.

5. Conclusions

Compression tests were performed on $\text{YBa}_2\text{Cu}_3\text{O}_{7-x}$ polycrystals with grain sizes of 3 and 7 μm at $1.3 \times 10^{-5}\text{s}^{-1}$ at temperatures from 1136–1253 K. The following results were obtained.

1. Steady-state deformation appears above 1203 K for both samples. The dislocation density of these samples is found to be very low.

2. The plots of the logarithm of steady-state stress as a function of T^{-1} are expressed by two straight lines for both grain sizes above 1203 K. From the slope of the straight lines, activation energies are determined to be approximately 150 kJ mol^{-1} , independent of grain size.

3. The strain-rate sensitivity of steady-state stress at various initial strain rates between 1.3×10^{-5} and $4 \times 10^{-4}\text{s}^{-1}$ in the temperature range 1203–1243 K gives a stress exponent of 1.3.

4. Work-hardening appears below 1203 K and dislocations with a high density are observed.

5. The results obtained on the compression tests and microstructural observations suggest that the dominant deformation mechanism is diffusional creep associated with grain-boundary sliding above 1203 K, and dislocation glide accompanied with grain-boundary sliding below 1203 K.

6. The grain growth is enhanced by deformation and is accompanied by development of strong anisotropy in grain shape and preferred arrangement.

References

1. S. N. SONG, Q. ROBINSON, D. L. JOHNSON and J. B. KETTERSON, *Solid State Commun.* **68** (1988) 391.
2. J. RABIER and M. F. DENANOT, *Rev. Phys. Appl.* **25** (1990) 55.
3. J. RABIER, in "Proceedings of the Japan–France Seminar on Lattice Defects in Ceramics", Tokyo, July 1989, JJAP series 2, p. 33.
4. T. HATANAKA and A. SAWADA, *Jpn J. Appl. Phys.* **28** (1989) L392.
5. *Idem, ibid.* **28** (1989) L794.
6. N. NARITA, H. HIGASHIDA and S. MISHINA, in "Proceedings of the 2nd International Symposium on Superconductors", Tsukuba 14–17, November (1989).
7. T. SUZUKI and S. TAKEUCHI, *Oyo Buturi* **58** (1989) 1743.
8. *Idem*, in "Proceedings of the Japan–France Seminar on Lattice Defects in Ceramics", Tokyo, July 1989, JJAP series 2, p. 9.
9. H. SAKA and K. KURODA, *Bull. Jpn. Inst. Metals* **29** (1990) 693.
10. H. SAKA, J. INAGAKI, T. YOSHIDA, T. MURASE and K. KURODA, in "Proceedings of the Japan–France Seminar on Lattice Defects in Ceramics", Tokyo, July 1989, JJAP series 2, p. 143.
11. P. E. REYES-MOREL, X. WU and I. W. CHEN, in "Ceramic Superconductors II", edited by M. F. Yan (American Ceramic Society Westerville, OH, 1988) pp. 590–7.
12. G. BUSSOD, A. PECHENIK, C. T. CHU and B. DUMN, *J. Am. Ceram. Soc.* **72** (1989) 137.
13. A. W. VON STUMBERG, N. CHEN, K. C. GORETTA and J. L. ROUBORT, *J. Appl. Phys.* **66** (1989) 2079.
14. K. C. GORETTA, J. L. ROUBORT, A. C. BIONDO, Y. GAO, A. R. de ARELLANO-LOPEZ and A. DOMINGUEZ-RODRIGUEZ, *J. Mater. Res.* **5** (1990) 2766.
15. W. J. KANG, K. YOSHIMI, S. HANADA, S. SAITO, Y. MURAYAMA, S. HAYASHI and A. NAGATA, *J. Appl. Phys.* **68** (1990) 6341.
16. T. M. SHAW, S. L. SHINDE, D. DIMOS, R. F. COOK, P. R. DUNCOMBE and C. KROLL, *J. Mater. Res.* **4** (1989) 248.
17. W. J. KANG, S. HANADA, A. NAGATA, and Y. WADAYAMA, *Mater. Sci. Eng. B*, in press.
18. "Metals Handbook", Vol. 8, 8th Edn (American Society for Metals) p. 42.
19. J. L. ROUBORT, *Acta Metall.* **27** (1979) 649.
20. T. YOSHIDA, K. KURODA and H. SAKA, *Philos. Mag. A* **62** (1990) 573.
21. O. A. KAIBYSHEV, R. M. IMAEV and M. F. IMAEV, *Sov. Phys. Dokl.* **34** (1989) 375.
22. R. VON MISES, *Z. Angew. Math. Mech.* **8** (1928).
23. T. B. LINDERMER, J. F. HUNLEY, J. E. GATES, A. L. SUTTON Jr, J. BRYNESTAD and C. R. HUBBARD, *J. Am. Soc.* **72** (1989) 1775.
24. K. KISHIO, J. SHIMOYAMA, T. HASEGAWA, K. KITAZAWA, and K. FUEKI, *J. Jpn Appl. Phys.* **26** (1987) L1228.

25. E. D. SPECHT, C. T. SPARKS, A. G. DHERE, J. BRYNOSTAD, O. B. CABIN, and D. M. KROEGER, *Phys. Rev. B* **37** (1988) 7426.
26. C. NAMGUNG, J. T. S. IRVINE, J. H. BINKS and A. R. WEST, *Supercond. Sci. Technol.* (1988) 169.
27. J. D. JORGENSEN, M. A. BENO, D. G. HINKS, L. SODERHOLM, K. J. VOLIN, R. L. HITTERMAN, J. D. GRACE and IVAN K. SCHULLER, *Phys. Rev. B* **36** (1987) 3608.
28. J. D. JORGENSEN, B. W. VEAL, W. K. KWOK, G. W. CRABTREE, A. UMEZAWA, L. J. NOWICKI and A. P. PAULIKAS, *ibid.* **36** (1987) 5731.
29. J. D. JORGENSEN, H. SHAKED, D. G. HINKS, B. DABROWSKI, B. W. VEAL, A. P. PAULIKAS, L. J. NOWICKI, G. W. GRABTREE, W. K. KWOK and L. H. NUNEZ, *Physica C* (1988) 578.

*Received 24 March 1992
and accepted 24 February 1993*